THE EUROPEAN
PHYSICAL JOURNAL C

# Borexino's search for low-energy neutrinos associated with gravitational wave events from GWTC-3 database

**Borexino Collaboration**

D. Basilico[1], G. Bellini[1], J. Benziger[2], R. Biondi[3,25], B. Caccianiga[1], F. Calaprice[4], A. Caminata[5], A. Chepurnov[6], D. D'Angelo[1], A. Derbin[7,8,a], A. Di Giacinto[3], V. Di Marcello[3], X. F. Ding[4,26], A. Di Ludovico[4,27], L. Di Noto[5], I. Drachnev[7], D. Franco[9], C. Galbiati[4,10], C. Ghiano[3], M. Giammarchi[1], A. Goretti[4,27], M. Gromov[6,11], D. Guffanti[12,28], Aldo Ianni[3], Andrea Ianni[4], A. Jany[13], V. Kobychev[14], G. Korga[15,16], S. Kumaran[17,18,29], M. Laubenstein[3], E. Litvinovich[8,19], P. Lombardi[1], I. Lomskaya[7], L. Ludhova[17,18], I. Machulin[8,19], J. Martyn[12], E. Meroni[1], L. Miramonti[1], M. Misiaszek[13], V. Muratova[7], R. Nugmanov[8,19], L. Oberauer[20], V. Orekhov[12], F. Ortica[21], M. Pallavicini[5], L. Pelicci[17,18], Ö. Penek[17,30], L. Pietrofaccia[4,27], N. Pilipenko[7], A. Pocar[22], G. Raikov[8], M. T. Ranalli[3], G. Ranucci[1,b], A. Re[1], N. Rossi[3], S. Schönert[20], D. Semenov[7], G. Settanta[17,31], M. Skorokhvatov[8,19], A. Singhal[17,18], O. Smirnov[11], A. Sotnikov[11], R. Tartaglia[3], G. Testera[5], E. Unzhakov[7], A. Vishneva[11], R. B. Vogelaar[23], F. von Feilitzsch[20], M. Wojcik[13], M. Wurm[12], S. Zavatarelli[5], K. Zuber[24], G. Zuzel[13]

1 Dipartimento di Fisica, Università degli Studi e INFN, 20133 Milan, Italy
2 Chemical Engineering Department, Princeton University, Princeton, NJ 08544, USA
3 INFN Laboratori Nazionali del Gran Sasso, 67010 Assergi (AQ), Italy
4 Physics Department, Princeton University, Princeton, NJ 08544, USA
5 Dipartimento di Fisica, Università degli Studi e INFN, 16146 Genoa, Italy
6 Lomonosov Moscow State University Skobeltsyn Institute of Nuclear Physics, Moscow 119234, Russia
7 St. Petersburg Nuclear Physics Institute NRC Kurchatov Institute, Gatchina 188350, Russia
8 National Research Centre Kurchatov Institute, Moscow 123182, Russia
9 APC, Université de Paris, CNRS, Astroparticule et Cosmologie, 75013 Paris, France
10 Gran Sasso Science Institute, 67100 L'Aquila, Italy
11 Joint Institute for Nuclear Research, Dubna 141980, Russia
12 Institute of Physics and Excellence Cluster PRISMA+, Johannes Gutenberg-Universität Mainz, 55099 Mainz, Germany
13 M. Smoluchowski Institute of Physics, Jagiellonian University, 30348 Kraków, Poland
14 Institute for Nuclear Research of NAS Ukraine, 03028 Kyiv, Ukraine
15 Department of Physics, Royal Holloway, University of London, Egham, Surrey TW20 OEX, UK
16 Institute of Nuclear Research (Atomki), Debrecen, Hungary
17 Institut für Kernphysik, Forschungszentrum Jülich, 52425 Jülich, Germany
18 RWTH Aachen University, 52062 Aachen, Germany
19 National Research Nuclear University MEPhI (Moscow Engineering Physics Institute), Moscow 115409, Russia
20 Physik-Department, Technische Universität München, 85748 Garching, Germany
21 Dipartimento di Chimica, Biologia e Biotecnologie, Università degli Studi e INFN, 06123 Perugia, Italy
22 Amherst Center for Fundamental Interactions and Physics Department, UMass, Amherst, MA 01003, USA
23 Physics Department, Virginia Polytechnic Institute and State University, Blacksburg, VA 24061, USA
24 Department of Physics, Technische Universität Dresden, 01062 Dresden, Germany
25 *Present address:* Max-Planck-Institut für Kernphysik, 69117 Heidelberg, Germany
26 *Present address:* IHEP Institute of High Energy Physics, Beijing 100049, China
27 *Present address:* INFN Laboratori Nazionali del Gran Sasso, 67010 Assergi (AQ), Italy
28 *Present address:* Dipartimento di Fisica, Universita degli Studi e INFN Milano-Bicocca, 20126 Milan, Italy
29 *Present address:* Department of Physics and Astronomy, University of California, Irvine, CA, USA
30 *Present address:* GSI Helmholtzzentrum für Schwerionenforschung GmbH, 64291 Darmstadt, Germany
31 *Present address:* Istituto Superiore per la Protezione e la Ricerca Ambientale, 00144 Rome, Italy

Springer

**Abstract** The search for neutrino events in correlation with gravitational wave (GW) events for three observing runs (O1, O2 and O3) from 09/2015 to 03/2020 has been performed using the Borexino data-set of the same period. We have searched for signals of neutrino-electron scattering and inverse beta-decay (IBD) within a time window of $\pm 1000$ s centered at the detection moment of a particular GW event. The search was done with three visible energy thresholds of 0.25, 0.8 and 3.0 MeV. Two types of incoming neutrino spectra were considered: the mono-energetic line and the supernova-like spectrum. GW candidates originated by merging binaries of black holes (BHBH), neutron stars (NSNS) and neutron star and black hole (NSBH) were analyzed separately. Additionally, the subset of most intensive BHBH mergers at closer distances and with larger radiative mass than the rest was considered. In total, follow-ups of 74 out of 93 gravitational waves reported in the GWTC-3 catalog were analyzed and no statistically significant excess over the background was observed. As a result, the strongest upper limits on GW-associated neutrino and antineutrino fluences for all flavors ($\nu_e$, $\nu_\mu$, $\nu_\tau$) at the level $10^9 - 10^{15}$ cm$^{-2}$ GW$^{-1}$ have been obtained in the 0.5–5 MeV neutrino energy range.

## 1 Introduction

The era of multi-messenger astronomy has started with the detection of gravitational waves (GW) by the LIGO experiment [1]. During O1 and O2 observing periods (09/2015–08/2017), LIGO/Virgo has detected 10 binary black-hole mergers and a single binary neutron-star merger [2]. Firstly, the short gamma-ray burst GRB170817A was detected in 1.7 s temporal interval coincidence with the GW170817 event from the binary neutron-star merger [3]. At present the third LIGO, Virgo and KAGRA Collaboration Gravitational Wave Transient Catalog (GWTC-3) consists of transient GW signal records discovered up to the end of LIGO-Virgo's third observing run (03) [4].

The observation of GW events triggered an intensive follow-up campaign in neutrino detectors [5–19]. Čerenkov neutrino telescopes (ANTARES, IceCube [5,10]) and Pierre Auger Observatory [6] have searched for high energy neutrinos above 100 GeV and 100 PeV, respectively. The experiment KamLAND has searched for inverse beta decay (IBD) antineutrino events within (1.8–111) MeV energy range [7,16] and the Super-Kamiokande collaboration has reported results for neutrino signals within 3.5 MeV to 100 PeV energy range [8,11,17]. The Borexino detector has searched for correlated neutrino events with visible energies above 0.25 MeV within a $\pm 500$ s time window centered at the detection

moment of the first three reported GW events in assumption of monochromatic and Fermi-Dirac spectra [9]. The Daya Bay collaboration has searched for possible electron-antineutrino signals with energies from 1.8 to 100 MeV in coincidence with 7 GW events including GW 170817 within three time windows of $\pm 10$, $\pm 500$, and $\pm 1000$ s relative to the occurrence of the GW events [13]. The XMASS-I 832 kg xenon detector has searched for event bursts associated with the 11 GW events detected during LIGO/Virgo's O1 and O2 periods [15]. The NOvA neutrino detectors have performed search for any signal coincident with 28 GW events and supernova like neutrino interactions in coincidence with 76 GW events [12,14]. The Baksan Underground Scintillation Telescope has searched for $\nu_\mu$ and $\bar\nu_\mu$ with energies above 1 GeV from the directions of the localization of the GW events and in temporal coincidence with the GW170817 occurring due to the merger of two neutron stars [18,19].

The neutrino and antineutrino events within a time window of $\pm 1000$ ($\pm 500$, $\pm 10$) s around the moment of gravitational wave detection were analyzed in the detectors mentioned above, but no evidence for an excess of coincident neutrino events had been reported. Combination of the data from gravitational, neutrino and electromagnetic detectors forms a new multi-messenger approach leading to a deeper understanding of astrophysical and cosmological processes through combination of information from different probes.

Here, we report the results of a search for signals with visible energy above 0.25 MeV in the Borexino detector in coincidence with GW events from GWTC-3. We look for neutrino signals from $\nu_e$, $\nu_{x=\mu,\tau}$ and antineutrinos $\bar\nu_e$, $\bar\nu_{x=\mu,\tau}$ originated in the GW events that scatter on electrons. We also search for signals of $\bar\nu_e$ that induce IBD reaction on protons.

Two different spectra of incoming neutrinos ($\nu_{e,x}$ and $\bar\nu_{e,x}$) were used for the analysis: the mono-energetic line and the spectrum expected from supernovae. The same $\bar\nu_e$-neutrino spectra were considered for search with the IBD reaction. The temporal correlation analysis between Borexino events and GW events were performed for three different merging modes of black holes and neutron stars – BHBH, NSNS, NSBH.

Negative results of searches for neutrino radiation accompanying GW events are presented as a limit on the neutrino or antineutrino fluences. In the papers above, the results of various detectors and different numbers of GW events were analyzed, sometimes the obtained limits of the neutrino fluence are normalized to the number of GW events. Since the data on the radiation mass and the distance to the event $R_i$ are available from the GWTC-3 catalog for almost all events, it would be natural, in assumption that the neutrino fluence has to be proportional to the radiation mass and inversely proportional to the square of $R_i$, to use this factor for comparison of the different experiments results.

[a] e-mail: derbin_av@pnpi.nrcki.ru (corresponding author)

[b] e-mail: spokesperson-borex@lngs.infn.it (corresponding author)

## 2 The Borexino detector

The Borexino is a liquid scintillator-based large volume detector specifically designed for neutrino detection. The experiment was located at the Laboratori Nazionali del Gran Sasso (LNGS) at the depth of 3800 m of water equivalent and has been operated since from May 2007 till October 2021. Such location provided good cosmic muon flux suppression by a factor of $\approx 10^6$. The detector structure represents an implementation of the graded shielding concept.

The water tank (WT) is constructed of stainless steel with high radiopurity and contains 2100 tons of ultra-pure water as additional shielding imposed to suppress external $\gamma$-rays and neutrons. The WT contains a stainless steel sphere (SSS) with radius of 6.75 m and thickness of 8 mm that serves as the scintillating inner detector body. The WT is equipped with 208 8-inch PMTs placed on its floor and outer surface of the SSS and is used as the Cherenkov muon veto (outer detector, OD) for identification of residual muons crossing the detector. The scintillation light is detected by nominally 2212 8-inch PMTs of the inner detector (ID) uniformly distributed on the inner surface of the SSS. The neutrino target consists of 278 tons ultra-pure organic liquid scintillator and is confined in the innermost detector part, that is divided by two 125 $\mu$m nylon "balloons", the Radon Barrier (RB) and the Inner Vessel (IV) with radii of 5.50 m and 4.25 m respectively.

The scintillator was chosen for the purpose of low-energy neutrino registration as pseudocumene (PC 1,3,4-trimethylbenzene, $C_6H_3(CH_3)_3$) doped with a fluorescent constituent PPO (2,5-diphenyloxazole, $C_{15}H_{11}NO$) in concentration of 1.5 g/l. The buffer volume serves as neutron and gamma radiation shield and is posed with a solution of a light quencher dope consisting of 2 g/l dimethylphthalate (DMP, $C_6H_4(COOCH_3)_2$).

Detection of charged particles in the Borexino detector occurs via production of the scintillator light in the scintillator volume and its detection by the PMTs. Since the moment the detector started operation until the end of the experiment, the number of active PMTs has decreased that is taken into account in the current analysis. The data are used for reconstruction of energy and spatial coordinates of an event and also allows identification a particle type ($e, \alpha, \mu$) due to differences in the scintillation time profiles.

Both energy and spatial resolutions of the detector were studied with radioactive sources placed at different positions inside the inner vessel. The energy and position resolutions are $\sigma_E \approx 50$ keV and $\sigma_X \approx 10$ cm at 1 MeV with 2000 PMTs, respectively; both are scaling with the energy of an event as $\sim 1/\sqrt{E}$ at low energies. The primary electronics of the Borexino detector is optimized for energies up to few MeV with energy calibration reliable up to 16.8 MeV. For the purpose higher energies operation the system of 96 fast waveform 400 MHz digitizers was developed, each of them is reading-in the signal summed from 24 PMTs. The Borexino detector is unable to determine directional information of a single event due to nearly isotropic emission of scintillation light (see, however, [20,21]).

A more detailed description of the Borexino detector can be found in the following papers [22–26].

Neutrinos $\nu_{e,x}$ and antineutrinos and $\bar{\nu}_{e,x}$ are detected by means of their elastic scattering on electrons:

$$\nu_{e,x}\ (\bar{\nu}_{e,x})\ +\ e^-\ \rightarrow\ \nu_{e,x}\ (\bar{\nu}_{e,x})\ +\ e^-. \tag{1}$$

For a given (anti)neutrino energy $E_\nu$, the maximum electron recoil energy $E_{emax}$ is given by the formula $E_{emax} = 2E_\nu^2/(2E_\nu + m_e)$ where $m_e$ is the electron mass.

Electron antineutrinos $\bar{\nu}_e$ can also be detected via the inverse beta-decay (IBD) reaction with an energy threshold of 1.8 MeV:

$$\bar{\nu}_e + p \rightarrow n + e^+. \tag{2}$$

The visible energy of the positron and two annihilation photons is related to the antineutrino energy as $E_{vis} = E_{\bar{\nu}_e} - 0.784$ MeV. The neutron capture on protons produces a delayed 2.22 MeV $\gamma$'s with mean capture time of $\sim 260\,\mu$s [27].

The Borexino was the first experiment that has detected and then precisely measured all solar neutrino fluxes (except for the $hep$-neutrino) [28–34] and has also registered antineutrinos emitted in decay of radionuclides naturally occurring within the Earth [38–41]. The Borexino detector is perfectly suited for the study of other fundamental problems, as well as searching for rare and exotic processes in particle physics and astrophysics [42–49]. Additionally, temporal correlations with transient astrophysical sources such as $\gamma$-ray bursts [50], gravitational wave events [9], solar flares [44], and fast radio burst [51] have been performed.

## 3 The Borexino data selection

The aim of data selection is to provide maximum exposure for the desired study with minimum background contribution. In the current analysis we search for neutrino-electron scattering, a reaction that has no specific interaction signature. Thus, the background has to be suppressed generically, as a reduction of the detector count rate per unit of exposure. Background composition of the Borexino experiment was carefully studied in the course of many years of research. In the current study we account for the following background component groups:

– Short-lived cosmogenic backgrounds ($\tau \leq 1$ s) such as $^{12}B$, $^8He$, $^9C$, $^9Li$ etc., and long-lived cosmogenic backgrounds ($\tau \geq 1$ s) such as $^{11}Be$, $^{10}C$, $^{11}C$ etc., produced within the detector fiducial volume.

– External backgrounds present in the material of the inner nylon vessel such as $^{210}$Pb and Uranium/Thorium decay chains.
– Internal natural backgrounds contained in the bulk of the detector fluid such as $^{14}$C, $^{85}$Kr, $^{210}$Bi and $^{210}$Pb.

These backgrounds can be suppressed by using information coming from the processed detector data such as spatial event distributions or ID/OD temporal and spatial coincidences. Cosmogenic backgrounds are reduced by applying the detector temporal veto after each muon, which could be discriminated through coincidence with outer veto as well as by pulse-shape discrimination [27]. A veto duration of 0.3 s after each muon crossing the IV is applied to suppress $^{12}$B to a statistically insignificant level and reduce $^{8}$He, $^{9}$C and $^{9}$Li by factor of 3 with a live time loss as small as 1 %. More long-lived cosmogenic backgrounds of $^{11}$C, $^{10}$C, $^{11}$Be and others can were not specifically suppressed by advanced veto system in order to save maximal exposure for neutrino events.

Backgrounds contained in the bulk of the detector can not be discriminated on event basis since they can not be localized neither spatially nor temporally. Nevertheless, the count rate of these background components are reduced by setting a cut on visible energy. This is important specifically due to the presence of $^{14}$C in the scintillator. $^{14}$C produces a beta-spectrum with an endpoint of 156 keV and has activity of roughly 110 Bq in the whole inner vessel.

The presence of this spectral component sets the lower threshold of the analysis to $E_1 = 0.25$ MeV of visible energy.[1] Two additional thresholds of $E_2 = 0.8$ and $E_3 = 3$ MeV of visible energy are applied for higher energy neutrino search. The second 0.8 MeV threshold was set in order to exclude $^{210}$Po and solar $^{7}$Be neutrino events and the third 3 MeV threshold rejects the most part of natural radioactivity. The threshold of 0.25 MeV allows to register neutrinos with energy as low as 0.4 MeV via $(\nu, e)$-elastic scattering.

Backgrounds contained in the nylon of IV can not be removed by any kind of purification and are therefore of the order of $10^2$–$10^3$ times higher than those within the bulk of the scintillator. The most important contributions come from $^{214}$Bi and $^{208}$Tl decays. These nuclides undergo $\beta$ and $\beta + \gamma$ decay processes with a continuous spectrum overlapping with the region of interest of the current analysis. The most effective way to suppress this kind of backgrounds is to perform a geometrical cut on events, selecting those within a fiducial volume. The fiducial volume is defined in such manner that all events within and further than 75 cm away from the IV are kept. The distance of 75 cm corresponds to 3 standard deviations of position reconstruction uncertainty at

the lowest 0.25 MeV energy threshold.[2] The corresponding fiducial volume has a mass of 145 t.

## 4 GW events, temporal window and neutrino spectra

We have used the GWTC-3 database compiled by the LIGO and VIRGO collaborations for O1, O2 and O3 observing runs [4]. This database contains information about possible sources of GW events, merger time of the event in GPS seconds, mass $M1$ and $M2$, chirp mass $\delta M$, final mass $M_f$ in solar mass units, red-shift $z$, and distance information $R$.

During the period of interest from September 2015 to March 2020, 93 GW events have been observed, 87 of which are black hole mergers(BHBH), 2 events of neutron star merge (NSNS) and 4 events of neutron star–black hole merge (NSBH).

The nearest GW event is the most famous merger of two neutron stars GW170817 occurred at $R = 40^{+7}_{-15}$ Mpc. The biggest redshift $z = 1.18^{+0.73}_{-0.53}$ ($R = 8280^{+6720}_{-4290}$ Mpc) was observed for GW190403-051519. This was the only GW event with red shift $z > 1$, while 90% of the GW events have $z < 0.64$.

We have considered the coincidence time window $\Delta t = 2000$ s centered at the GW observation time with a width of $\pm 1000$ s covering a possible delay of sub-MeV neutrinos propagating at the sublight speed. Negative interval of time window $\Delta t = 0 \ldots -1000$ s covers earlier emission of neutrinos in the case of binary mergers [52]. For a distance corresponding to the $z = 0.64$ redshift, the delay will reach 1000 s in case of 0.6 MeV neutrinos with a rest mass of 65 meV, which is the upper limit on the heaviest neutrino mass state from the Planck 2018 data [53] and oscillation mass squared differences [54]. All selected GW events had the data taking time above 95% of the corresponding time interval $\Delta t$.

There's no expectation of MeV neutrino emission from BHBH mergers, since no ordinary matter is present. Neutrinos could only be produced either by some exotic scenario or if the GW event were misidentified and was actually either a supernova or a merger including neutron star. Since there is no reliable theory for the low-energy part of the neutrino emission spectrum for BHBH mergers, we calculated fluence limits for two different kinds of possible neutrino spectra: the monoenergetic line and the supernovae low-energy continuous spectrum $\Phi(E_\nu)$. The latter was assumed to be quasi-thermal spectrum with mean energy $\langle E \rangle$ and deviation from thermal distribution characterized by the pinching parameter $\alpha = 3$ for all neutrino flavors $(\nu_{e,x}, \bar{\nu}_{e,x})$ [55–57]. The emitted neutrino spectrum $S(E_\nu)$ depends on the neutrino energy

---

[1] Visible energy spectrum of $^{14}$C is broadened up to this value due to energy resolution of the detector.

[2] Position reconstruction precision increases with energy due to statistical reasons.

$E_\nu$ as:

$$\Phi(E_\nu) \sim (E_\nu/T)^\alpha e^{(-E_\nu/T)}, \qquad (3)$$

where $T = \langle E \rangle / (\alpha + 1)$ is effective temperature, which was considered to be the same for all neutrino flavors.

The expected number of events depends on neutrino spectrum and $(\nu, e)$-scattering cross section $d\sigma(E_\nu)/dE_e$ [58]. The total cross section $\sigma(E_a, E_b)$ for electron with energy in the range $(E_a, E_b)$ is obtained by integrating the $d\sigma(E_\nu)/dE_e$ over recoil electron energies $E_e$ between the electron energies $E_a$ and $E_b$:

$$\sigma(E_a, E_b) = \int \frac{d\sigma(E_\nu, E_e)}{dE_e} dE_e \qquad (4)$$

If the neutrino spectrum $\Phi(E_\nu)$ is not a monochromatic line, the total cross section for the electron recoil energy interval $(E_1, E_2)$ is calculated as:

$$\sigma(E_a, E_b) = \int \int \frac{d\sigma(E_\nu, E_e)}{dE_e} \Phi(E_\nu) dE_e dE_\nu \qquad (5)$$

Additionally, in order to compare the theoretical cross sections (4) and (5) with the experimental results, finite energy resolution of the detector has to be taken into account [50]. The neutrino-electron cross sections, the number of electrons in the Borexino fiducial volume and the GW neutrino fluences will determine the expected number of neutrino events in the detector.

## 5 Analysis of the temporal correlations of Borexino signals with GW events

The Borexino detector was in data taking mode when 70 (out of 87) black hole mergers, 2 neutron star mergers and 2 (out of 4) neutron star black hole mergers have been occurred. Three different variants of binary merges in temporal coincidence with the Borexino data were analyzed separately. Some parameters of GW events involving neutron stars as obvious possible source of the neutrino flux are shown in Table 1. Additionally, average values of the these parameters for 70 BHBH mergers are shown in the bottom row of Table 1.
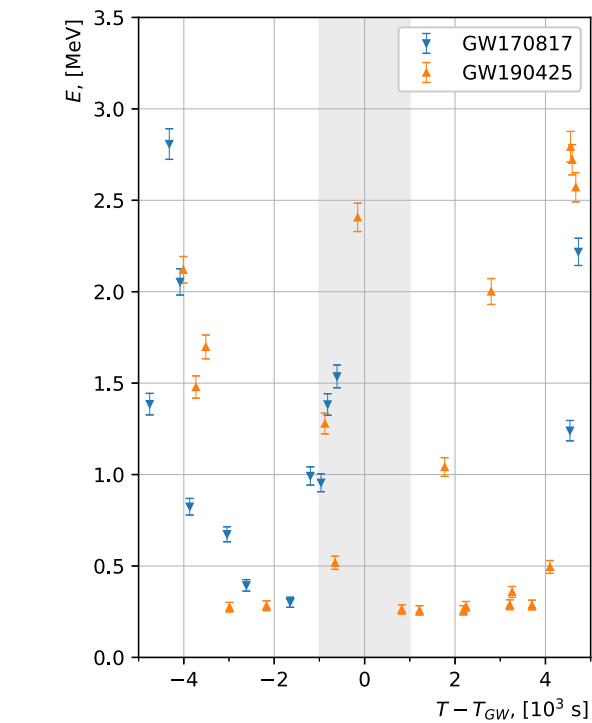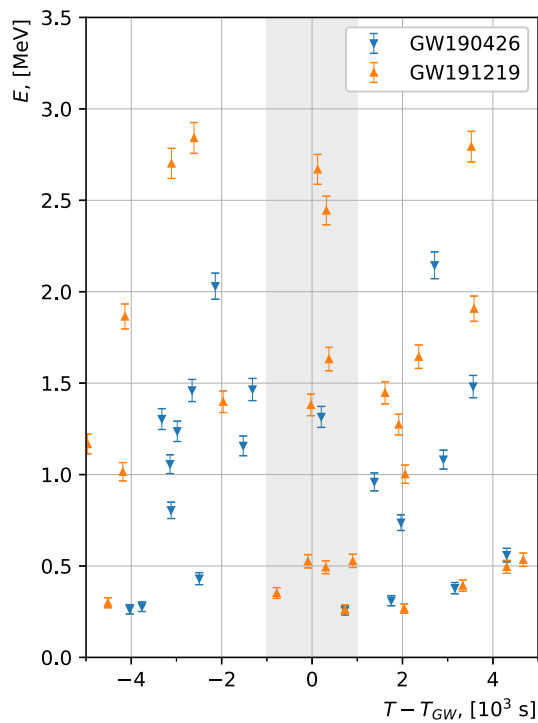


**Fig. 1** Borexino events with energies above 0.25 MeV occurring within ± 5000 s of GW170817 (blue inverted triangles) and GW190425 (yellow triangles) events produced by the coalescence of two neutron stars. All events are consistent with the expected rates of solar neutrinos and background events

For the possible registration of neutrinos, the most interesting is the GW170817 signal measured on 2017 August 17 produced by the coalescence of two neutron stars with masses 1.46 $M_\odot$ and 1.27 $M_\odot$ and occurred at a record close distance $R = 40^{+7}_{-15}$ Mpc. The second registered neutron star merger GW190425 event occurred at a distance 4 times greater with the close chirp mass, which determines the amplitude of the GW signal.

The detection time and energy of Borexino events passing all data selection cuts in ± 5000 s windows around GW170817 and GW190425 events due to the merger of two neutron stars are shown in Fig. 1. The closest events with energies 1.54 (2.41) MeV occurred at 610 (154) s before

**Table 1** GW events involving neutron stars, for which the temporal correlation analysis was carried out with the Borexino signals. $M1$ and $M2$ are masses in solar mass units $M_\odot$, $R$ is distance in Mpc, $M^{rad}$ is radiative mass in $M_\odot$ units. Average values of $M1$, $M2$, $R$ and $M^{rad}$ are given for 70 black hole mergers

| GW event | Mode | $M1$ | $M2$ | $R$ | $M^{rad}$ |
|---|---|---|---|---|---|
| GW 170817 | NSNS | 1.46 | 1.27 | 40 | $\leq 0.04$ |
| GW 190425 | NSNS | 2.0 | 1.40 | 160 | – |
| GW 190426 | NSBH | 5.7 | 1.5 | 370 | – |
| GW 191219 | NSBH | 31.1 | 1.17 | 550 | 0.1 |
| 70 GW BHs | BHBH | 36.7 | 23.0 | 2130 | 2.4 |

**Fig. 2** Borexino events with energies above 0.25 MeV occurring within $\pm 5000$ s of GW190426 (blue inverted triangles) and GW191219 (yellow triangles) events produced by the coalescence of neutron star and black hole
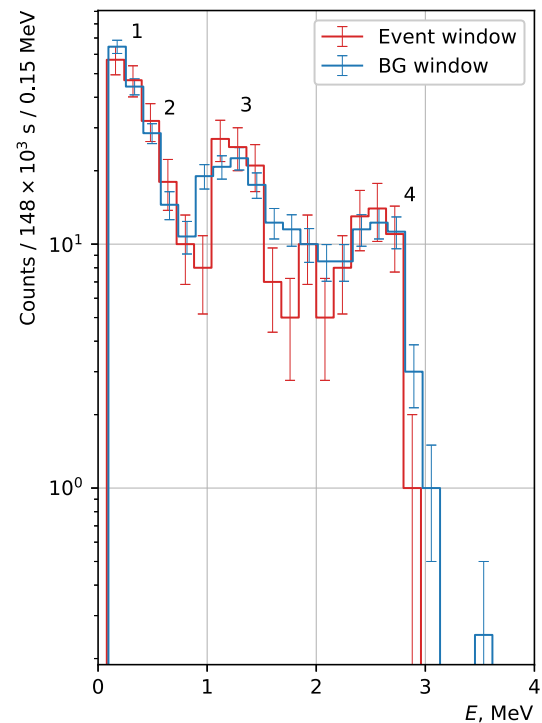


**Fig. 3** Borexino visible energy spectrum of singles in correlation with 70 BHBH GW events in the $\pm 1000$ s time window (red line with errors). Blue line shows the normalized background spectrum measured in $[-5000 \dots -1000]$ s and $[1000 \dots 5000]$ s intervals. 1 – $^{210}$Po $\alpha$-peak, 2 – recoiled electrons from the solar $^7$Be-neutrino, 3 – $^{11}$C $\beta^+$-decay, 4 – external background ($^{208}$Tl)

GW170817 (GW190425), respectively. A similar Fig. 2 shows Borexino events for two GW190426 and GW191219 events corresponding to the merger of a neutron star and a black hole.

Number of Borexino events in $\pm 1000$ s interval with energy above 0.25 MeV ($N_1$) and 0.8 MeV ($N_2$) in comparison with the reduced backgrounds defined for intervals $[-5000 \dots -1000, 1000 \dots 5000]$ s are shown in Table 2 for 4 GW events involving neutron stars. One can see that no excess of the counting rate, associated with GW events involving neutron stars, above the expected background is observed. So, there are only 3 events in the $\pm 1000$ s interval centered at the GW170817 event arrival time with the energy in the 0.25-−16.8 MeV range, while $2.5 \pm 0.8$ solar neutrino

and background reduced events were obtained within the $[-5000 \dots -1000, 1000 \dots 5000]$ s window. All detected events were in agreement with expected solar neutrino and background count rates.

The energy spectrum of Borexino events in correlation with BHBH GW events in the $\pm 1000$ s time window for 150 keV interval and the normalized background spectrum of events registered in $[-5000 \dots -1000]$ s and $[1000 \dots 5000]$ s intervals are shown in Fig. 3.

Number of events and the reduced background in $\pm 1000$ s interval with energy above 0.25 MeV and 0.8 MeV for 70 GW BHBH events are shown in Table 2. No statistically signif-

**Table 2** Number of events $N_1$ and $N_2$ in $\pm 1000$ s interval with energies above 0.25 MeV and 0.8 MeV, correspondingly, for GW events involving neutron stars. For comparison the reduced backgrounds $B_1$ and $B_2$ defined for intervals $[-5000 \dots -1000, 1000 \dots 5000]$ s are also shown. The same data for 70 BHBH GW events is shown in the last column

| GW mode | 170817 NSNS | 190425 NSNS | 190426 NSBH | 191219 NSBH | 70 GWs BHBH |
|---|---|---|---|---|---|
| $N_1$ | 3 | 4 | 2 | 9 | 304 |
| $B_1$ | $2.5 \pm 0.8$ | $4.3 \pm 1.0$ | $4.8 \pm 1.1$ | $4.3 \pm 1.1$ | $310 \pm 9$ |
| $N_2$ | 3 | 2 | 1 | 4 | 158 |
| $B_2$ | $1.8 \pm 0.7$ | $2.0 \pm 0.7$ | $2.8 \pm 0.8$ | $3.0 \pm 0.9$ | $163 \pm 7$ |

icant excess of the difference between these spectra for any energy interval was observed.

The spectrum in Fig. 3 is dominated by $^{14}$C in the region below 0.250 MeV of visible energy, by the recoil electrons from solar $^7$Be neutrinos in 0.25-−0.8 MeV interval, by cosmogenic $^{11}$C in 1–2 MeV region and by external gamma-quanta of $^{214}$Bi and $^{208}$Tl in 2–3 MeV region. All these components can not be significantly reduced by any available data selection techniques without serious exposure loss. Figure 3 shows the energy spectrum in the range 0.25-−4.0 MeV and only three events were detected with energies above 4 MeV.

Based on the spectrum of the Borexino detector in Fig. 3 three mentioned above energy thresholds $E_{1,2,3}$ are selected for the analysis. The analysis is performed for the energy intervals from $E_{1,2,3}$ to $E_{emax}$, the latter must not exceed the range of validity of the detector energy response calibration (0.25-−16.8) MeV. In the analysis, the energy resolution of the detector $\sigma(E_e)$ is taken into account [50]. We calculated the overall number of candidate events above $E_{1,2,3}$ in the ± 1000 interval for various values of neutrino energy $E_\nu$ or average energy $\langle E \rangle$ for supernova spectra.

Since there is no statistically significant excess of the number of events within ± 1000 s GW window above the background, the upper limits on fluences $\Phi_{\nu_{e,x},\bar{\nu}_{e,x}}$ for mono-energetic (anti)neutrinos with the energy $E_\nu$ are calculated as:

$$\Phi_{\nu_{e,x},\bar{\nu}_{e,x}} = \frac{N_{90}(E_\nu, n_{\mathrm{obs}}, n_{\mathrm{bkg}})}{r N_e \sigma(E_{\mathrm{th}}, E_{e_{\max}})}, \qquad (6)$$

where $E_{th} = E_{1,2,3}$, $N_{90}(E_\nu, n_{obs}, n_{bkg})$ is the 90% C.L. upper limit for the number of GW-correlated events in the $(E_{th}, E_{emax})$ interval per single GW and $N_e$ is the number of electrons in 145 t of the Borexino scintillator. The limits were obtained in assumption that the whole neutrino fluence consists of only one individual flavor. The factor $\sigma(E_{th}, E_{emax})$ represents the cross section for detected neutrinos ($\nu_{e,x}$, $\bar{\nu}_{e,x}$) with the energy $E_\nu$ without oscillations while recoil electrons are detected in the interval $(E_{th}, E_{emax})$ taking into account the detector energy resolution [50]. The recoil electron detection efficiency $r$ was taken as 1, with the accuracy corresponding to the precision of the fiducial volume definition ($\simeq 1\%$ [34]).

The numerator $N_{90}(E_\nu, n_{obs}, n_{bkg})$ was calculated for spectra of coincident (in ± 1000 s) and non-coincident events in the energy interval $(E_{th}, E_{emax})$. Here, $n_{obs}$ and $n_{bkg}$ denote overall numbers of observed and background events in this energy interval normalized by their respective times. The longer interval $\Delta t_{bkg}$ =18 ks for background detection was chosen in order to reduce the error of $n_{bkg}$ that plays an important role in the analysis. The value $n_{bkg}$ was normalized by the overall time ratio taking into account the actual live time of the detector within these time windows.
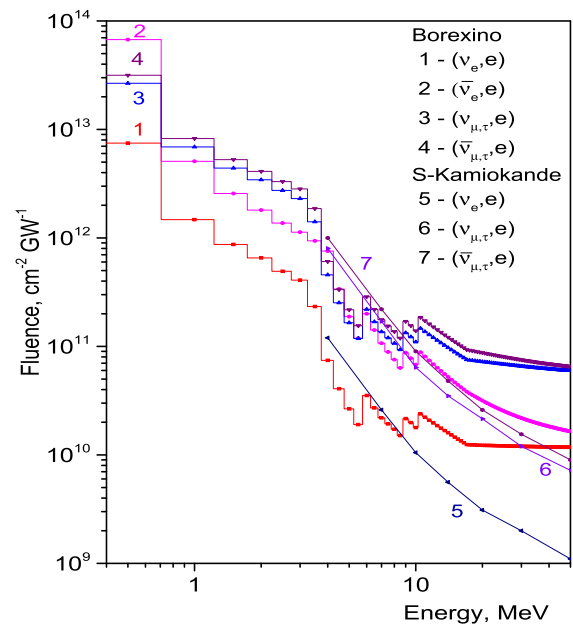


**Fig. 4** Borexino upper limits on mono-energetic neutrino fluences obtained with $(\nu, e)$ elastic scattering reaction through the temporal correlation analysis for 74 GW events (90% C.L.): 1-$\nu_e$, 2-$\bar{\nu}_e$, 3-$\nu_{\mu,\tau}$, 4-$\bar{\nu}_{\mu,\tau}$. The limits 5, 6 and 7 of Super-Kamiokande obtained for single GW170817 event from $(\nu, e)$-scattering reaction are also shown [11]

The procedure was repeated for neutrino energies $E_\nu$ from 0.5 MeV to 50 MeV in increments of 0.5 MeV. As was mentioned above, in order to have the best ratio of the expected effect with respect to the background and taking into account the shape of the spectrum (Fig. 3) the three energy thresholds $E_1$, $E_2$ and $E_3$ were used for different neutrino energies. The analysis is performed in the energy interval $(E_{1,2,3}, E_{emax})$ if $E_{emax}$ is not exceeded the range of the detector energy calibration, in the later case the value 16.8 MeV was used for the right border of the analysis interval.

For the case of all 74 GW events the upper limits on neutrino and antineutrino fluences of different flavors normalized per single GW are shown in Fig. 4. The jumps in the upper limit at the energies above 7 MeV is associated with the inclusion of the above-mentioned three events with energies above 4 MeV in the analysis. The limits change weakly at higher neutrino energies above 17 MeV due to the fact that the maximum energy of recoil electrons $E_{emax}$ is constrained by the value 16.8 MeV in the analysis. These are the first constraints on the fluence of neutrino with energy below 4 MeV obtained from the neutrino-electron scattering reaction. The previous limits obtained by Super-Kamiokande collaboration for the GW170817 NSNS merger with $(\nu_{e,x}, e)$- and $(\bar{\nu}_x, e)$-scattering are also shown in the Fig. 4 [11].

For the case of supernovae spectrum with a mean energy with a mean energy $\langle E \rangle = 15.6$ MeV and the parameter $\alpha = 3$ (Eq. 3) and integrating over the analyzed electron recoil energy interval $E_{1,2,3} - 16.8$ MeV, we get the lim-

**Table 3** Upper limits on fluences from all 74 events per single GW for all neutrino flavors obtained from the temporal correlation analysis in $10^9$ cm$^{-2}$ units (90% C.L.) calculated for mono-energetic neutrinos and the supernova spectrum with $\langle E \rangle = 15.6$ MeV. The limits in the right column obtained through the study of IBD reaction

| $E_\nu$ | $\Phi_{\nu_e}$ | $\Phi_{\bar{\nu}_e}$ | $\Phi_{\nu_{\mu,\tau}}$ | $\Phi_{\bar{\nu}_{\mu,\tau}}$ | $\Phi_{\bar{\nu}_e}$ IBD |
|---|---|---|---|---|---|
| 2 | 650 | 1800 | 3400 | 4100 | 100 |
| 6 | 35 | 200 | 220 | 290 | 1.7 |
| 10 | 18 | 68 | 110 | 140 | 0.51 |
| 14 | 16 | 52 | 97 | 120 | 0.25 |
| 18 | 12 | 36 | 74 | 91 | – |
| 30 | 12 | 22 | 66 | 75 | – |
| 50 | 12 | 17 | 60 | 66 | – |
| $\langle 15.6 \rangle$ | 12 | 19 | 63 | 71 | 0.48 |
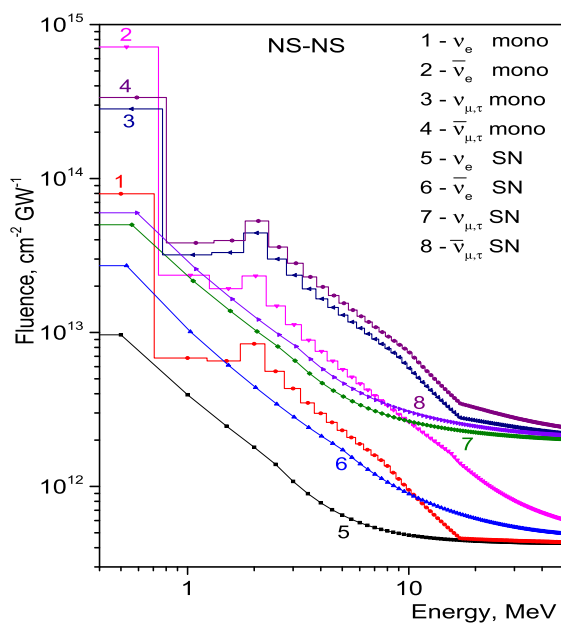


**Fig. 5** The merger of two neutron stars – GW170817 event. The upper limits on the fluences of monoenergetic neutrinos (mono): 1-$\nu_e$, 2-$\bar{\nu}_e$, 3-$\nu_{\mu,\tau}$, 4-$\bar{\nu}_{\mu,\tau}$ and neutrinos with supernova spectra (SN): 5-$\nu_e$, 6-$\bar{\nu}_e$, 7-$\nu_{\mu,\tau}$, 8-$\bar{\nu}_{\mu,\tau}$ (90% C.L.). The x-scale shows the energy of monoenergetic neutrinos $E_\nu$ or the average energy $\langle E \rangle$ in the case of a supernova spectrum
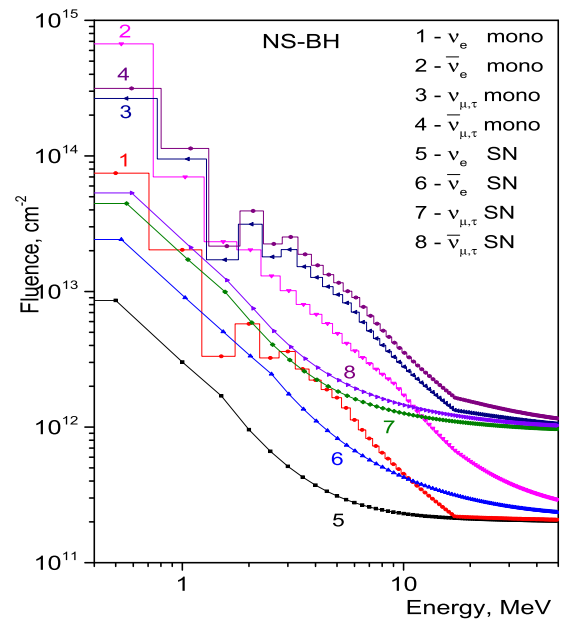


**Fig. 6** The merger of neutron star and black hole – GW190426 and GW191219 events. The upper limits on the fluences of monoenergetic neutrinos (Energy $= E_\nu$): 1-$\nu_e$, 2-$\bar{\nu}_e$, 3-$\nu_{\mu,\tau}$, 4-$\bar{\nu}_{\mu,\tau}$ and neutrinos with supernova spectra (Energy=$\langle E \rangle$): 5-$\nu_e$, 6-$\bar{\nu}_e$, 7-$\nu_{\mu,\tau}$, 8-$\bar{\nu}_{\mu,\tau}$ (90% C.L.)

its on the total electron neutrino fluence per single GW: $\Phi(\nu_e) \leq 1.2 \times 10^{10}$ cm$^{-2}$ (90% C.L.) that is close to the limit obtained for mono-energetic neutrinos with the same energy. The values of the limits on other neutrino flavors obtained from the $(\nu, e)$-scattering channel are given in Table 3. We also calculated the upper limit on the electron antineutrinos ($\bar{\nu}_e$) fluence given in Table 3 using the IBD reaction (see Sect. 8).

## 6 Limits on neutrino fluences from GW events involving neutron stars

The limits on $\nu_{e,x}$ and $\bar{\nu}_{e,x}$ fluence were alternatively obtained for NSNS and NSBH GW events. The intervals for the analysis ($E_{1,2,3}$, $E_{emax}$) are set to the same way as previously described. The values of the monoenergetic neutrino energy $E_\nu$ and the supernova neutrino mean energy $\langle E \rangle$ from 0.5 to 50 MeV in increments of 0.5 MeV, the expected spectra of recoil electrons and the number of detected events in the interval ($E_{1,2,3}$, $E_{emax}$) were used in the calculations.

The relation (6) was converted into the obtained fluence limits for all neutrino flavors given in Fig. 5 for NSNS GW 170817 event and in Fig. 6 for NSBH GW 190426 and GW 191219 events, both for mono-energetic neutrinos and for supernova neutrinos. We only analyzed the first NSNS GW 170817 event separately, since the second NSNS GW 190425 event occurred at a distance 4 times further, and the exactly GW 170817 event was analyzed by almost all of the above-mentioned neutrino detectors.

At neutrino energies above 17 MeV, the limits become almost constant since the $(\nu, e)$-scattering cross section is proportional to $E_\nu$ and the spectrum of recoil electrons weakly depends on the electron energy.

The results for the NSNS case are also shown in Table 4 for mono-energetic neutrinos. In case of the supernova neutrino spectrum, the fluence constraints are slightly stronger than the monoenergetic neutrino limit at $\langle E \rangle = E_\nu$ (Table 5). The wide expected neutrino spectrum allows to set limits at energies $\langle E \rangle \geq 16.8$ MeV.

**Table 4** Borexino 90% C.L. upper limits for the fluences of all neutrino flavours from NSNS GW 170817 event, obtained through the study of $(\nu, e)$ elastic scattering of monoenergetic neutrinos and IBD reaction. $E_\nu$ is given in MeV units, $\Phi_{\nu_{e,x}, \bar{\nu}_{e,x}}$ – in $10^{12}$ cm$^{-2}$ units

| $E_\nu$ | $\Phi_{\nu_e}$ | $\Phi_{\bar{\nu}_e}$ | $\Phi_{\nu_{\mu,\tau}}$ | $\Phi_{\bar{\nu}_{\mu,\tau}}$ | $\Phi_{\bar{\nu}_e}$ IBD |
|---|---|---|---|---|---|
| 2 | 8.4 | 23 | 44 | 53 | 3.8 |
| 6 | 1.9 | 4.7 | 11 | 13 | 0.062 |
| 10 | 0.95 | 2.6 | 5.9 | 7.4 | 0.019 |
| 14 | 0.59 | 1.8 | 3.6 | 4.5 | 0.0090 |
| 18 | 0.46 | 1.3 | 2.8 | 3.4 | – |
| 30 | 0.44 | 0.81 | 2.4 | 2.8 | – |
| 50 | 0.44 | 0.61 | 2.2 | 2.4 | – |

**Table 5** Borexino 90% C.L. upper limits for the fluences of all neutrino flavours from NSNS GW 170817 event, obtained through the study of $(\nu, e)$ elastic scattering of neutrino with supernova spectrum and IBD reaction. $\langle E \rangle$ is given in MeV units, $\Phi_{\nu_{e,x}, \bar{\nu}_{e,x}}$ – in $10^{12}$ cm$^{-2}$ units

| $\langle E \rangle$ | $\Phi_{\nu_e}$ | $\Phi_{\bar{\nu}_e}$ | $\Phi_{\nu_{\mu,\tau}}$ | $\Phi_{\bar{\nu}_{\mu,\tau}}$ | $\Phi_{\bar{\nu}_e}$ IBD |
|---|---|---|---|---|---|
| 2 | 1.8 | 4.4 | 10 | 12 | 1.7 |
| 6 | 0.58 | 1.4 | 3.4 | 4.0 | 0.12 |
| 10 | 0.48 | 0.89 | 2.7 | 3.0 | 0.046 |
| 14 | 0.46 | 0.73 | 2.4 | 2.7 | 0.040 |
| 18 | 0.45 | 0.65 | 2.3 | 2.5 | 0.037 |
| 30 | 0.43 | 0.55 | 2.1 | 2.3 | 0.069 |
| 50 | 0.43 | 0.50 | 2.0 | 2.2 | 0.21 |



**Fig. 7** The upper limits on the neutrino fluences from 26 most intensive HBHB merges. The mono-energetic neutrinos (Energy=$E_\nu$): 1-$\nu_e$, 2-$\bar{\nu}_e$, 3-$\nu_{\mu,\tau}$, 4-$\bar{\nu}_{\mu,\tau}$. The neutrinos with supernova spectra (Energy=$\langle E \rangle$): 5-$\nu_e$, 6-$\bar{\nu}_e$, 7-$\nu_{\mu,\tau}$, 8-$\bar{\nu}_{\mu,\tau}$. (all for 90% C.L.)

## 7 Limits on the neutrino fluences from the selected most intensive BHBH GW events

Since for almost all GW events the distance to the event $R_i$ and the radiation mass $M_i^{rad}$ are known (with some accuracy), in contrast to gamma-ray bursts or fast radio bursts cases [50,51], it is possible to obtain the limit on the neutrino fluence for some hypothetical standard event at a fixed distance and with a known radiative mass. This allows to compare the obtained limits on the neutrino fluence for a different set of GW events. The neutrino fluence from i-th GW event assuming isotropic emission is proportional:

$$\Phi_i = \frac{\epsilon M_i^{rad} c^2}{4\pi R_i^2 \langle E_i \rangle}, \tag{7}$$

where $\epsilon$ is a fraction of neutrino radiation and $\langle E_i \rangle$ is the average neutrino energy. The obtained limits on the neutrino fluences can be converted to the limit on the value of $\epsilon$.

According to the GWTC-3 database for 70 BHBH GW events when the Borexino detector was in data taking mode, the distances to events $R_i$ lie in the range (0.3–8.3 Gpc) and an average distance is $\langle R_i \rangle = 2.1$ Gpc. The corresponding radiative masses $M_i^{rad}$ are inside (0.3–9.4) $M_\odot$ interval with average mass $\langle M_i^{rad} \rangle = 2.6 M_\odot$. Therefore, as a reference event, we define the "standard" event with $M^{rad}$ equals one solar mass $M_\odot$ at a distance of one Gpc. The upper limits on the neutrino fluence obtained for the single GW event $\Phi_i$ can be converted to the limit on the fluence from "standard" GW event as $\Phi_{std} = w_i \Phi_i$ where the weight $w_i = (1 \text{ Gpc}/R_i)^2 (M_i^{rad}/M_\odot)$.

Among 70 BHBH GW events, we selected 26 events, for which weight $w_i$ is greater than 1. For these 26 events, the average distance is 1.0 Gpc, the average radiative mass is 2.3 $M_\odot$, and the factor characterizing the neutrino flux $\langle w_{26} \rangle = 3.1$. Correspondingly, for the remaining 44 events, the average distance is 2.8 Gpc, the radiative mass is 2.9 $M_\odot$, and the factor $\langle w_{43} \rangle = 0.44$. These 26 most intense events were used to search for an additional contribution to the $\pm 1000$ s temporal interval from the neutrino interactions, the spectrum was represented as mono-energetic neutrinos and neutrinos with a supernova spectrum. Since no statistically significant excesses were found, the resulting upper limits on the neutrino fluences for all flavors are shown in the Fig. 7. Although the upper bounds on the fluences for mono-energetic neutrinos in Fig. 7 (line 1–4) turn out to be weaker than in Fig. 4, they are obtained for GW events with the expected most intense neutrino fluxes.
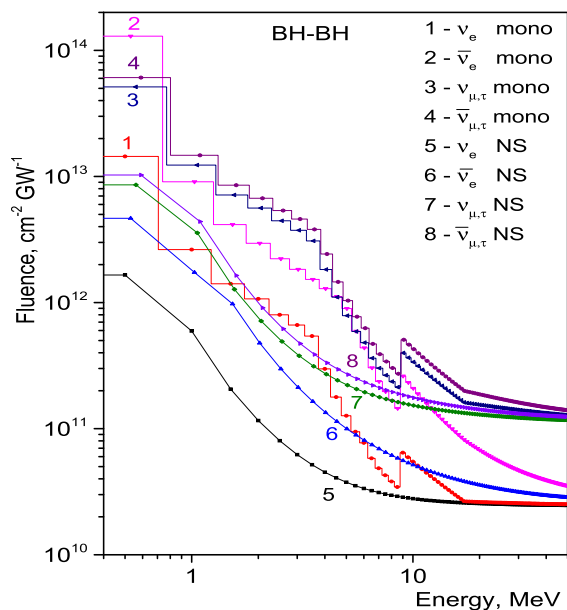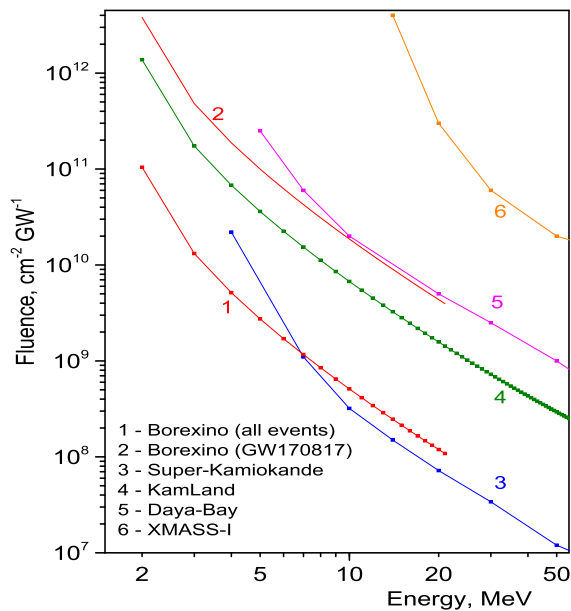
**Fig. 8** Upper limits on the fluence of mono-energetic electron antineutrinos $\bar{\nu}_e$ obtained using IBD reaction. 1 – Borexino (all 74 GW events, reduced per single GW event), 2 – Borexino (GW 170817 NSNS event), 3 – Super-Kamiokande coll. [11] (GW 170817), 4 – KamLand coll. [16] (GW 170817), 5 – DayaBay coll. [13], 6 – XMASS-I coll. [15] (all for 90% C.L.)

## 8 Limits on the $\bar{\nu}_e$-fluence from the IBD reaction

As already mentioned, electron antineutrinos can be also detected in the Borexino detector via inverse $\beta$-decay (IBD) reaction on protons with energy threshold of $E_{\bar{\nu}_e} = 1.8$ MeV. The cross section of this process is much higher than the one for $(\bar{\nu}_e, e)$ elastic scattering. Additionally, the IBD offers a unique signature given by temporal and spatial coincidence of two correlated events associated with detection of a positron and a neutron. The prompt positron event with visible energy of $E_{\bar{\nu}_e} - 0.784$ MeV accompanied by $\gamma$-rays from neutron capture mostly on protons or carbon nuclei with a small probability. As a result, the rate of the events selected as IBD candidates is much lower with respect to the rate of single electron-like events.

The procedure of IBD events selection and the energy spectrum of prompt positron events are described in detail in [39–41,43,44]. In the IBD analysis, we used the same 16.8 MeV upper boundary of the visible energy range as in the case of the $(\nu, e)$-scattering analysis. No IBD events were observed in the $\pm 1000$ s interval around the selected GW events and the expected background was almost zero [41,44] that allowed us to use the conservative value of $N_{90}(E_\nu, n_{\text{obs}}, n_{\text{bkg}}) = 2.44$ in the analysis [59]. Since the cross section of IBD reaction is about two orders of magnitude larger than $(\nu, e)$-scattering cross sections at given neutrino energies, and the background level is smaller, the most

stringent upper limits have been obtained for the fluence of electron antineutrinos.

The upper limit on the mono-energetic electron antineutrinos ($\bar{\nu}_e$) fluence using the IBD reaction is calculated from the relation (6) but with replacing of the $N_e$ with the number of protons $N_p$ and considering the cross section of IBD reaction [60]. The resulting limit on $\bar{\nu}_e$ fluence for 74 GW events reduced per one GW event is shown in Fig. 8 (line 1) and Tables 3, 4 and 5. For comparison, the limit on $\bar{\nu}_e$ fluence for one GW event (e.g. GW170817 NSNS merge) is presented by line 2 in Fig. 8.

Upper limits on the fluence can be converted into upper limits on the total energy radiated in form of neutrinos $\epsilon M_i^{rad}$ for a BHBH, NSNS and NSBH mergers using relation (7). We consider only the energy radiated by 10 MeV electron neutrinos $\nu_e$ and antineutrinos $\bar{\nu}_e$ under assumption of isotropic angular distribution of emitted neutrinos. Upper limits on the fluence of $\nu_e$ and $\bar{\nu}_e$ from the closest NSNS GW 170817 event obtained for $(\nu_e, e)$-scattering and from IBD reaction (4) lead to restrictions on $\epsilon M^{rad} c^2 \leq 2.9 \times 10^{60}$ erg and $\epsilon M^{rad} c^2 \leq 5.7 \times 10^{58}$ erg, accordingly. These values can be compared with the energy of solar mass $M_\odot c^2 = 1.8 \times 10^{54}$ erg. Accordingly, the restrictions on fraction of neutrino radiation become unnatural and exceed unity ($\epsilon_{\nu_e} \leq 1.0 \times 10^9$ and $\epsilon_{\bar{\nu}_e} \leq 2.0 \times 10^7$). For comparison, we note that if GW170817 event occurred at the same distance as the supernova collapse SN1987A at 51 kpc from Earth, the sensitivity to the energy released in form of 10 MeV neutrinos would be $\epsilon M^{rad} c^2 \leq 8.9 \times 10^{52}$ erg (0.05 $M\odot$) and $\epsilon_{\bar{\nu}_e} \leq 1.2$.

In the case of 26 most intensive BHBH GW events, the resulting fluence is:

$$\Phi_{tot} = \sum_{i=1}^{26} \frac{\epsilon M_i^{rad} c^2}{4\pi R_i^2 \langle E_i \rangle}. \qquad (8)$$

where the upper limit on the total fluence $\Phi_{tot} = 1.45 \times 10^{12}$ cm$^{-2}$ (Fig. 7) and values $M_{rad_i}$ and $R_i$ can be taken from the GWTC-3 database. Since for 26 GW events the average mass $\langle M^{rad} \rangle = 11 M_\odot$ as well as the average squared distance $\langle R^2 \rangle = 0.5$ Gpc$^2$ are about 300 times larger than for the GW 170817 event, the upper limits of the value of $\epsilon_{\nu_e, \bar{\nu}_e}$ are of the same order as for obtained with GW 170917 event.

This suggests that successful detection of low-energy neutrinos should be possible only in case of anisotropic angular distribution of neutrino emission. The limits on energy radiated into neutrinos of other flavors can be easily calculated from Tables 3, 4 and 5.

## 9 Conclusion

We have searched for signals of neutrino-electron scattering with visible energies above 250 keV within a time window

of $\pm 1000$ s centered at the detection moment of a particular GW event. Two types of incoming neutrino spectra were considered: a mono-energetic line and supernova neutrino spectrum given by modified Fermi-Dirac distribution for different effective neutrino temperatures. We searched for coincident neutrino-electron elastic scattering of $\nu_{e,\mu,\tau}$ and $\bar{\nu}_{e,\mu,\tau}$ and IBD of $\bar{\nu}_e$ in the Borexino detector with the 74 GW events associated with the O1, O2 and O3 observing runs of the LIGO/VIRGO detectors. We looked for an excess in the number of Borexino events produced by neutrino-electron elastic scattering and the inverse beta-decay on protons correlated to 74 GW events from the GWTC-3 database. We found no statistically significant increase in the number of events, with visible energies above 0.25 MeV within time windows of $\pm 1000$ s centered at the moment of GW arrival for all three options for merging of black holes and neutron stars. As a result, new limits on the fluence of monochromatic and supernova neutrinos of all flavors were set for neutrino energies in range of 0.5–5 MeV. Also, the inverse beta-decay reaction was considered in order to set a new limit on the fluence of electron antineutrinos related with the GW events.

**Data Availability Statement** This manuscript has no associated data or the data will not be deposited. [Authors' comment:...].

### References

1. B.P. Abbott et al. [LIGO Scientific Coll. and Virgo Coll.], Observation of gravitational waves from a binary black hole merger. Phys. Rev. Lett. **116**, 061102 (2016)
2. B.P. Abbott et al. [LIGO Scientific Coll. and Virgo Coll.], GWTC-1: a gravitational-wave transient catalog of compact binary mergers observed by LIGO and Virgo during the first and second observing runs. Phys. Rev. X **9**, 031040 (2019)
3. B.P. Abbott et al. [LIGO Scientific Coll. and Virgo Coll.], GW170817: observation of gravitational waves from a binary neutron star inspiral. Phys. Rev. Lett. **119**, 161101 (2017)
4. GWTC-3: compact binary coalescences observed by LIGO and Virgo during the second part of the third observing run. arXiv:2111.03606v2
5. S. Adrian-Martinez et al. [ANTARES and IceCube coll.], High-energy neutrino follow-up search of gravitational wave event GW150914 with ANTARES and IceCube. Phys. Rev. D **93**, 122010 (2016)
6. A. Aab et al., Ultrahigh-energy neutrino follow-up of gravitational wave events GW150914 and GW151226 with the Pierre Auger Observatory. Phys. Rev. D **94**, 122007 (2016)
7. A. Gando et al [KamLAND coll.], A search for electron antineutrinos associated with gravitational wave events GW150914 AND GW151226 using Kamland. Astrophys. J. **829**, L34 (2016) [A. Gando et al., Erratum: "A Search for Electron Antineutrinos Associated with Gravitational-wave Events GW150914 and GW151226 Using KamLAND" Astrophys. J. 851 (2017) L22]
8. K. Abe et al. [Super-Kamiokande coll.], Search for neutrinos in Super-Kamiokande associated with gravitational wave events GW150914 AND GW151226. Astrophys. J. **830**, L11 (2016)
9. M. Agostini et al. [Borexino coll.], A search for low-energy neutrinos correlated with gravitational wave events GW 150914, GW 151226, and GW 170104 with the borexino detector. Astrophys. J. **850**, 21 (2017)
10. A. Albert et al., Search for high-energy neutrinos from binary neutron star merger GW170817 with ANTARES, IceCube, and the Pierre Auger Observatory. Astrophys. J. **850**, L35 (2017)
11. K. Abe et al., Search for neutrinos in super-Kamiokande associated with the GW170817 neutron-star merger. Astrophys. J. **857**, L4 (2018)
12. M.A. Acero et al., Search for multimessenger signals in NOvA coincident with LIGO/Virgo detections. Phys. Rev. D **101**, 112006 (2020)
13. F.P. An et al [Daya Bay Coll.], Search for electron-antineutrinos associated with gravitational-wave events GW150914, GW151012, GW151226, GW170104, GW170608, GW170814, and GW170817 at Daya Bay. Chin. Phys. C **45**, 055001 (2021)
14. M.A. Acero et al., Extended search for supernovalike neutrinos in NOvA coincident with LIGO/Virgo detections. Phys. Rev. D **104**, 063024 (2021)
15. K. Abe et al. [XMASS-I coll.], Search for event bursts in XMASS-I associated with gravitational-wave events. Astropart. Phys. **129**, 102568 (2021)
16. K. Abe et al., Search for low-energy electron antineutrinos in KamLAND associated with gravitational wave events. Astrophys. J. **909**, 116 (2021). arXiv:2012.12053v1
17. K. Abe et al.,Search for neutrinos in coincidence with gravitational wave events from the LIGO-Virgo O3a Observing Run with the Super-Kamiokande detector. Astrophys. J. **918**(2), 78 (2021). arXiv:2104.09196
18. M.M. Boliev et al., Search for muon neutrinos from the gravitational wave event GW170817 at the Baksan Underground Scintillation Telescope. J. Phys. Conf. Ser. **1787**, 012034 (2021)
19. V.B. Petkov et al., Searching for muon neutrinos from regions of the localization of gravitational-wave events. Bull. Russ. Acad. Sci. Phys. **85**, 444 (2021)
20. M. Agostini et al. [Borexino coll.], First directional measurement of sub-MeV solar neutrinos with Borexino. Phys. Rev. Lett. **128**(9), 091803 (2022)
21. M. Agostini et al. [Borexino coll.], Correlated and integrated directionality for sub-MeV solar neutrinos in Borexino. Phys. Rev. D **105**(5), 052002 (2022)

22. G. Alimonti et al. [Borexino Collaboration], Science and technology of Borexino: a real-time detector for low energy solar neutrinos. Astropart. Phys. **16**, 205 (2002)

23. G. Alimonti et al. [Borexino Collaboration], The Borexino detector at the Laboratori Nazionali del Gran Sasso. NIMA **600**, 568 (2009)

24. H. Back et al. [Borexino Collaboration], Borexino calibrations: hardware, methods, and results. JINST **7**, P10018 (2012)

25. G. Bellini et al. [Borexino Collaboration], Final results of Borexino Phase-I on low-energy solar neutrino spectroscopy. Phys. Rev. D **89**, 112007 (2014)

26. M. Agostini et al. [Borexino Collaboration], Simultaneous precision spectroscopy of pp, 7Be, and pep solar neutrinos with Borexino Phase-II. Phys. Rev. D **100**, 082004 (2019)

27. G. Bellini et al. [Borexino Collaboration], Muon and cosmogenic neutron detection in Borexino. JINST **6**, P05005 (2011)

28. C. Arpesella et al. [Borexino Collaboration], Direct measurement of the 7Be solar neutrino flux with 192 days of Borexino data. Phys. Rev. Lett. **101**, 091302 (2008)

29. G. Bellini et al. [Borexino Collaboration], Precision measurement of the 7Be solar neutrino interaction rate in Borexino. Phys. Rev. Lett. **107**, 141302 (2011)

30. G. Bellini et al. [Borexino Collaboration], Measurement of the solar 8B neutrino rate with a liquid scintillator target and 3 MeV energy threshold in the Borexino detector. Phys. Rev. D **82**, 033006 (2010)

31. M. Agostini et al. [Borexino Collaboration], Improved measurement of 8B solar neutrinos with 1.5 kt y of Borexino exposure. Phys. Rev. D **101**, 062001 (2020)

32. G. Bellini et al. [Borexino Collaboration], First evidence of pep solar neutrinos by direct detection in borexino. Phys. Rev. Lett. **108**, 051302 (2012)

33. G. Bellini et al. [Borexino Collaboration], Neutrinos from the primary proton-proton fusion process in the Sun. Nature **512**, 383 (2014)

34. M. Agostini et al. [Borexino Collaboration], Comprehensive measurement of pp-chain solar neutrinos. Nature **562**, 505 (2018)

35. M. Agostini et al. [Borexino Collaboration], Experimental evidence of neutrinos produced in the CNO fusion cycle in the Sun. Nature **587**, 577 (2020)

36. M. Agostini et al. [Borexino Collaboration], Sensitivity to neutrinos from the solar CNO cycle in Borexino. Eur. Phys. J. C **80**, 1091 (2020)

37. S. Appel et al. [Borexino Collaboration], Improved measurement of solar neutrinos from the carbon-nitrogen-oxygen cycle by Borexino and its implications for the Standard Solar Model. Phys. Rev. Lett. **129**, 252701 (2022)

38. G. Bellini et al. [Borexino Collaboration], Observation of geoneutrinos. Phys. Lett. B **687**, 299 (2010)

39. G. Bellini et al. [Borexino Collaboration], Measurement of geoneutrinos from 1353 days of Borexino. Phys. Lett. B **722**, 295 (2013)

40. M. Agostini et al. [Borexino Collaboration], Spectroscopy of geoneutrinos from 2056 days of Borexino data. Phys. Rev. D **92**, 031101(R) (2015)

41. M. Agostini et al. [Borexino Collaboration], Comprehensive geoneutrino analysis with Borexino. Phys. Rev. D **101**, 012009 (2020)

42. G. Bellini et al. [Borexino Collaboration], Absence of a day-night asymmetry in the 7Be solar neutrino rate in Borexino. Phys. Lett. B **707**, 22 (2012)

43. G. Bellini et al. [Borexino Collaboration], Study of solar and other unknown anti-neutrino fluxes with Borexino at LNGS. Phys. Lett. B **696**, 191 (2011)

44. M. Agostini et al. [Borexino Collaboration], Search for low-energy neutrinos from astrophysical sources with Borexino. Astropart. Phys. **125**, 102509 (2021)

45. S.K. Agarwalla et al. [Borexino Collaboration], Constraints on flavor-diagonal non-standard neutrino interactions from Borexino Phase-II The Borexino Collaboration. J. High Energy Phys. **2020**, 38 (2020)

46. G. Bellini et al. [Borexino Collaboration], New experimental limits on the Pauli-forbidden transitions in 12C nuclei obtained with 485 days Borexino data. Phys. Rev. C **81**, 034317 (2010)

47. G. Bellini et al. [Borexino Collaboration], Search for solar axions produced in the p(d,3He)A reaction with Borexino detector. Phys. Rev. D **85**, 092003 (2012)

48. M. Agostini et al. [Borexino Collaboration], New limits on heavy sterile neutrino mixing in 8B decay obtained with the Borexino detector. Phys. Rev. D **88**, 072010 (2013)

49. M. Agostini et al. [Borexino Collaboration], A test of electric charge conservation with Borexino. Phys. Rev. Lett. **115**, 231802 (2015)

50. M. Agostini et al. [Borexino Collaboration] Borexino's search for low-energy neutrino and antineutrino signals correlated with gamma-ray bursts. Astropart. Phys. **86**, 11 (2017)

51. S. Appel et al. [Borexino Collaboration], Search for low-energy signals from fast radio bursts with the Borexino detector Eur. Phys. J. C **82**, 278 (2022)

52. B. Baret, I. Bartos, B. Bouhou et al., Bounding the time delay between high-energy neutrinos and gravitational-wave transients from gamma-ray bursts. Astropart. Phys. **35**, 1 (2011)

53. N. Aghanim et al. [Planck collaboration], Planck 2018 results. VI. Cosmological parameters. arXiv:1807.06209

54. I. Esteban, M.C. Gonzalez-Garcia, A. Hernandez-Cabezudo, M. Maltoni, T. Schwetz, Global analysis of three-flavour neutrino oscillations: synergies and tensions in the determination of the mass ordering. JHEP **01**, 106 (2019). arXiv:1811.05487

55. I. Tamborra, B. Muller, L. Hudepohl, H.T. Janka, G. Raffelt, High-resolution supernova neutrino spectra represented by a simple fit. Phys. Rev. D **86**, 125031 (2012). arXiv:1211.3920

56. C. Lujan-Peschard, G. Pagliaroli, F. Vissani, Spectrum of supernova neutrinos in ultra-pure scintillators. J. Cosmol. Astropart. Phys. JCAP **07**, 051 (2014)

57. A. Mirizzi, I. Tamborra, H. Janka, N. Saviano, K. Scholberg, R. Bollig, L. Hudepohl, S. Chakraborty, Supernova neutrinos: production, oscillations and detection. Riv. Nuovo Cim. **39**, 1 (2016). arXiv:1508.00785

58. J.N. Bahcall, M. Kamionkowski, A. Sirlin, Solar neutrinos: radiative corrections in neutrino-electron scattering experiments. Phys. Rev. D **51**, 6146 (1995)

59. G.J. Feldman, R.D. Cousins, Unified approach to the classical statistical analysis of small signals. Phys. Rev. D **57**, 3873 (1998)

60. A. Strumia, F. Vissani, Precise quasielastic neutrino/nucleon cross section. Phys. Lett. B **564**, 42 (2003)